UNEC Journal of Engineering and Applied Sciences
Vol. 4, No.2, 2024, pp. 12-19
DOI: https://doi.org/10.61640/ujeas.2024.1202

SECTION:
CHEMISTRY &
MATERIALS SCIENCE

Synthesis and structural characterization of new complexes based on silver nanoparticles, diphenylcarbazide, and cetyltrimethylammonium bromide

A.A. Imamaliyeva*, F.V. Hajiyeva, F.M. Chiragov

Baku State University, Department of Chemistry, 23 Z. Xalilov st., Baku Az 1148, Azerbaijan
email: *aytenimamaliyeva@hotmail.com*

Abstract

In this work, the synthesis of new complexes based on silver nanoparticles (AgNP), diphenylcarbazide reagent (DPC), and cetyltrimethylammonium bromide (CTAB) was carried out, and the optimal conditions for their production were determined. The structures of the synthesized binary DPC+Ag and ternary DPC+Ag+CTAB complexes were studied using X-ray diffraction (XRD), infrared (IR), and ultraviolet (UV) spectroscopy. From the UV analysis, it was observed that the maximum peaks of the DPC reagent are found at wavelengths of 235 nm, 262 nm, 308 nm, and 345 nm, corresponding to the π-π* transition of the C-C bond and the n-π* transition between the C=N groups. Due to the surface plasmon resonance of the binary complex, new peaks in the absorption spectra were identified at wavelengths of 248 nm, 288 nm, 315 nm, and 355 nm. In the ternary complex, peaks in the absorption band were observed at wavelengths of 305 nm and 348 nm. The spectroscopic properties of DFC and its binary and ternary complexes were investigated through IR analyses. The aromatic C-H bonds of the phenyl group appear in the range of 3000-3100 cm^{-1}, while the C=C bonds of the phenyl group appear around 1500-1600 cm^{-1}. The peaks corresponding to the carbonyl (C=O) bond of the carbazide group are found in the range of 1650-1700 cm^{-1}, and the peaks related to the N-H groups appear around 1500-1600 cm^{-1}. The interaction of DFC with AgNPs was examined by analyzing shifts and changes in intensity of the IR spectroscopy absorption bands.

***Keywords*:** Silver, nanoparticle, CTAB, complex, reagent, DPC.
PACS numbers: 62.23.St, 78.67.Bf, 81.07.-b, 81.07.Wx, 81.16.-c

Received:	*Revised:*	*Accepted:*	*Published:*
18 October 2024	*20 November*	*26 November 2024*	*26 December 2024*

1. Introduction

In recent times, nanomaterials have attracted the attention of the scientific community due to their unique properties and various technological applications. The different properties of nanoscale materials compared to macroscale materials often result from size limitations, the dominance of interfacial processes, and quantum effects. These new and distinctive properties of nanostructured materials lead to improvements in catalyst efficiency, tunable photoactivity, power enhancement, and many other intriguing characteristics [1]. Silver nanoparticles (AgNPs) of various shapes are widely used in biomedical imaging as optical labels and substrates for surface-enhanced Raman spectroscopy due to their optical properties, particularly localized surface plasmon resonance. The characteristics of AgNPs, which vary significantly according to shape and size, are crucial for these applications. Many studies demonstrate that the surface plasmon resonance (SPR) of Ag nanoparticles fundamentally depends on the number and position of peaks, size, and dielectric environment of the metal

nanoparticles [2]. Metal nanoparticles are characterized by high conductivity, a large surface-to-volume ratio, and plasmonic properties [3-4]. SPR properties enable the amplification and manipulation of light at the nanoscale level, thereby enhancing the sensitivity and resolution of optical devices. Among various metal nanoparticles, silver (Ag) is widely studied due to its high permeability, excellent light absorption, high sensitivity, resolution, antibacterial activity, and chemical stability [5-7].

Diphenylcarbazide (DPC) is a widely used reagent in analytical chemistry, primarily due to its ability to form colored complexes with various metal ions [8-11]. With the chemical formula $C_{12}H_{11}N_3O$, diphenylcarbazide is a derivative of carbazide in which two phenyl groups are substituted at the nitrogen atom. This organic compound is utilized as an indicator for iron titration and in the colorimetric determination of Cr (VI). DPC contains two amino groups that can interact with the surface of nanoparticles through hydrogen bonding. In this work, we utilize DPC as a selective ligand to modify silver nanoparticles for the determination of various metals.

The purpose of this article is to study the synthesis and structure of new complexes based on silver nanoparticles, diphenylcarbazide reagent, and cetyltrimethylammonium bromide (CTAB), which can be effective in the determination of many elements using photometric and other methods in analytical chemistry.

2. Experiments

1.1.Materials

Silver nitrate (AgNO3, PLC 141459, 98% chemically pure), soluble starch ((C6H10O5)n, PLC 121096, 98% chemically pure), β-D glucose (C6H12O6, CAS No.50-99-7, 98% chemically pure); sodium hydroxide (NaOH, PLC 141687, 98% chemically pure), cetyltrimethylammonium bromide (CTAB, AB 117004, 98% chemically pure), ethanol (C2H5OH, CAS No.64-17-5, 95% chemically pure.), diphenyl carbazide DPC (CAS140-22-7), 98% chemically pure) were used as received.

1.2.Synthesis of Ag Nanoparticles

The synthesis and stabilization of Ag nanoparticles were carried out in the following steps: First, 150 mL of a 1% starch solution was added to 100 mL of a 0.01 M $AgNO_3$ solution. Next, 100 mL of a 0.07 M sodium hydroxide solution was mixed with 100 mL of a 0.2 M glucose solution. This prepared NaOH and glucose solution was then added to the $AgNO_3$ and starch mixture and stirred for 30 minutes. Immediately after this process, the solution turned dark brown, indicating the formation of a colloidal solution of Ag nanoparticles. Then, to clean the Ag nanoparticles from extraneous and unreacted ions, the nanoparticles are separated in an R 5430 Eppendorf ultracentrifuge at 12,000 rpm for 30 minutes and washed several times with in equal volume ratios of water and ethanol. This process was performed under ambient conditions.In this synthesis process, starch serves as both a reducing agent and a stabilizer, while NaOH acts as a reaction accelerator. Glucose also functions as a reducing agent.

1.3. Synthesis of Ag+DPC+CTAB-Based Complex

In this work, the synthesis of new complexes based on silver nanoparticles, diphenylcarbazide (DPC) reagent, and cetyltrimethylammonium bromide (CTAB) was carried out. First, a 10^{-3} M concentration solution of the DPC reagent was prepared in a 1:1 water-alcohol mixture. To this, 10 mL of the pre-prepared 0.01 M Ag nanoparticles solution was added to 50 mL of the 10^{-3} M DPC reagent and stirred on a magnetic stirrer for 2 hours. The color of the resulting solution changed from dark red to red, indicating the formation of a binary complex. For the synthesis of the ternary complex, an additional 10 mL of the 0.01 M Ag nanoparticles solution was added to 50 mL of the 10^{-3} M DPC reagent and stirred for an

additional 2 hours. After this, 5 mL of a 0.5% (0.01 M) CTAB solution was added, and stirring continued to obtain the ternary complex. The obtained binary and ternary complexes are dried by heating in a muffle furnace at 120 degrees for 3 hours to remove any residual solvent and moisture.CTAB acts as a stabilizer in the complex formation process, ensuring the stability of the silver nanoparticles with the reactants

Research Methods

Ultraviolet spectra of the samples were obtained using a SPECORD 210 PLUS spectrophotometer (Analytic Jena, Germany) at wavelengths ranging from 200 to 900 nm at room temperature. The infrared (IR) spectra of the samples were measured with a Varian 640 infrared spectrometer at wavelengths of 400 to 4000 cm^{-1}, also at room temperature. X-ray analysis of the reagent and complexes was conducted at room temperature using a Rigaku Mini flex 600 diffractometer (Japan).

3. Results and discussion

X-ray analysis, including techniques like X-ray diffraction (XRD), is widely used to investigate the crystalline structure of materials, determine atomic arrangements, bond lengths, and angles, as well as to analyze nanostructures, phase compositions, and structural defects [11-16].

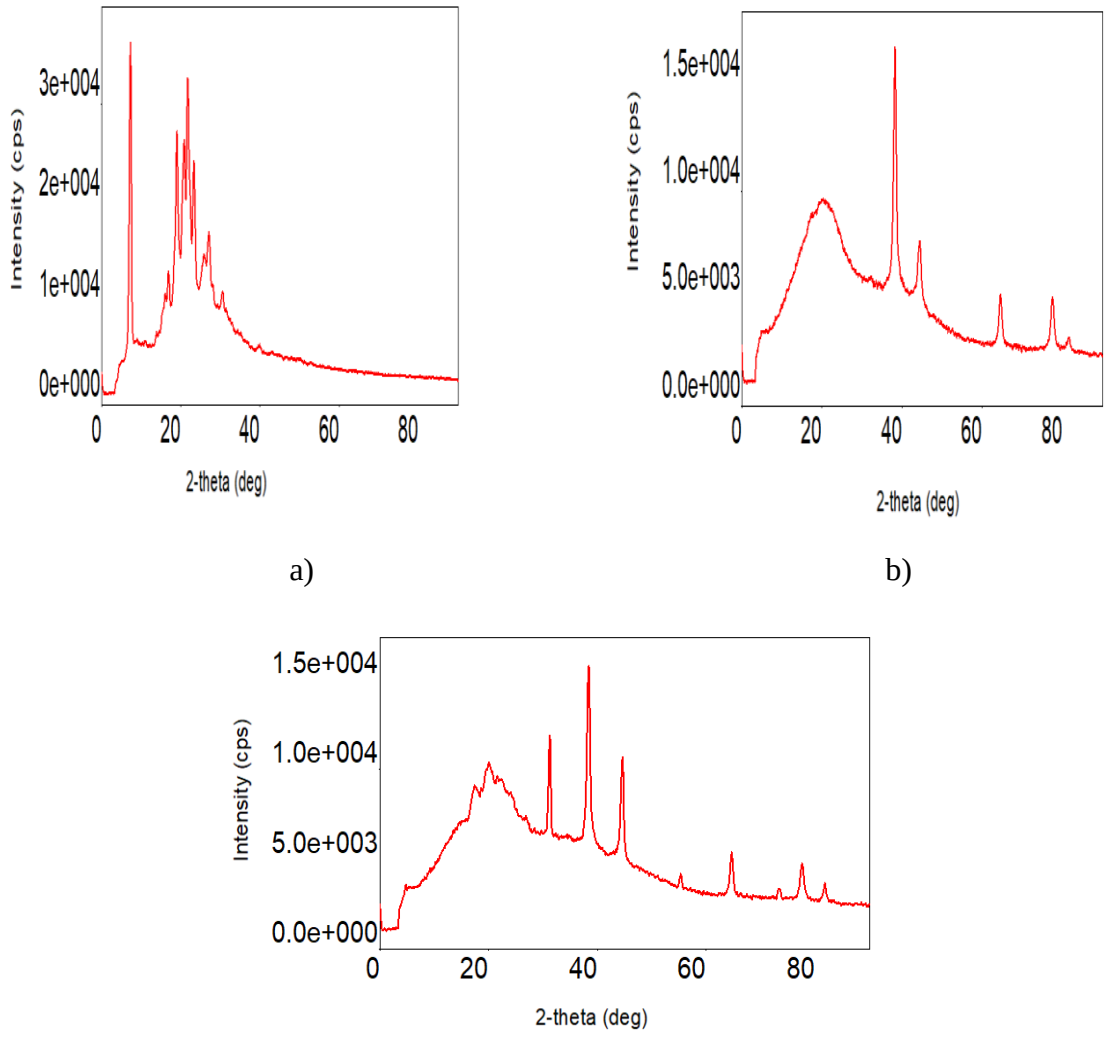

Figure 1. XRD diffractograms of DPC reagent (a), DPC+Ag (b) and DPC+Ag+CTAB (c) complexes.

Figure 1 shows the XRD diffractograms of the DFC reagent (a), DPC+Ag binary complex (b), and DPC+Ag+CTAB ternary complex (c). The crystallite sizes of the reagent, binary, and ternary complexes were calculated using the Debye-Scherrer formula (1) :

$$D = \frac{K\lambda}{\beta COS\theta} \quad (1)$$

where K is a unitless constant (K=0.94), λ is the wavelength of the incident X-ray (λ=1.5406 Å, Cu Kα), θ is the angle corresponding to the diffraction maximum, and β is the full width at half maximum (FWHM). According to the XRD diffractograms, the average size of the crystallites in the DPC reagent is 16.06 nm, while in the DPC+Ag binary complex- 11.42 nm and the DPC+Ag+CTABr ternary complex, it is 13.65 nm. In the XRD diffractogram of the DPC+Ag binary complex, peaks are observed at 2θ angles of 38.21°, 44.36°, 64.47°, 77.43°, and 81.54°. For the DPC+Ag+CTABr ternary complex, maxima appear at 2θ angles of 31.15°, 38.35°, 44.57°, 55.30°, 64.65°, 73.39°, 77.58°, and 81.77°.

DPC			DPC+Ag			DPC+Ag+CTAB		
2θ	β	D, nm	2θ	β	D, nm	2θ	β	D, nm
1.47^0	9.1	0.90	38.21^0	0.771	11.39	31.15^0	0.331	26.03
7.40^0	0.518	16.06	44.36^0	1.05	8.540	38.35^0	0.644	13.65
15.91^0	1.42	5.9	64.47^0	0.86	11.41	44.57^0	0.600	14.95
16.81^0	0.62	13.53	77.43^0	0.90	11.82	55.30^0	0.40	23.43
18.97^0	0.75	11.22	81.54^0	0.61	17.96	64.65^0	0.60	16.36
20.80^0	0.97	8.7				73.39^0	0.49	21.119
21.62^0	0.82	10.30				77.58^0	0.75	14.2
23.26^0	0.65	13.04				81.77^0	0.52	21.11
25.59^0	1.92	4.43						
27.0^0	0.61	14						
30.50^0	0.82	10.49						

Table 1. Data of DPC reagent, DPC+Ag double and DPC+Ag+CTAB triple complexes estimated by X-ray diffractometry method.

IR Spectroscopy provides information about the characteristic vibrations of functional groups in compounds and helps analyze their molecular structure [17-21]. Diphenylcarbazide, also known as diphenylcarbazone, has the chemical formula $C_{13}H_{11}N_3O$. The IR spectrum allows for the identification of functional groups such as aromatic rings, carbonyl groups, and carbazide moieties in diphenylcarbazide. Its structure features two phenyl rings connected by a carbazide group. The aromatic C-H bonds of the phenyl group appear as sharp peaks at around 3000-3100 cm^{-1}, corresponding to the stretching of C-H bonds in the aromatic system. The C=C bonds in the phenyl group produce peaks in the range of about 1500-1600 cm^{-1}, which are also sharp. Peaks around 1300-1400 cm^{-1} correspond to the C-N bonds of the carbazide group, reflecting the interaction of the carbazide group with the phenyl rings. Changes in these peaks during the formation of the binary and ternary complexes indicate the establishment of coordination interactions between the carbazide group and silver nanoparticles (AgNPs). Peaks around 1650-1700 cm^{-1} correspond to the carbonyl (C=O) bond of the carbazide group, indicating the presence of a carbonyl functional group. The intensity of this peak changes during the formation of the binary complex, suggesting coordination of the carbonyl group with the silver nanoparticles. Additionally, peaks related to the N-H groups appear around 1500-1600 cm^{-1}.

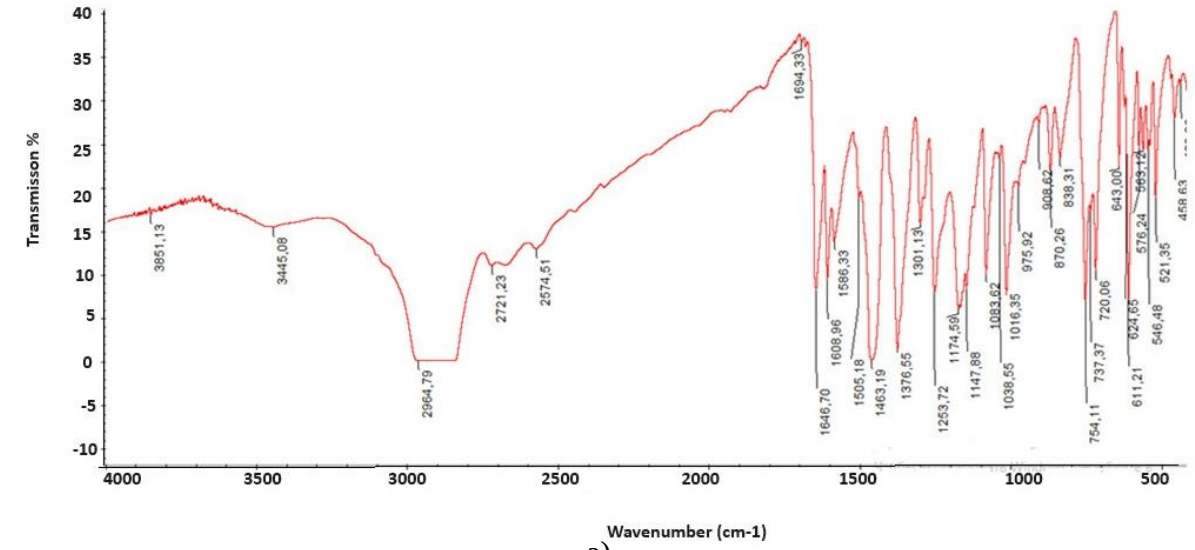

a)

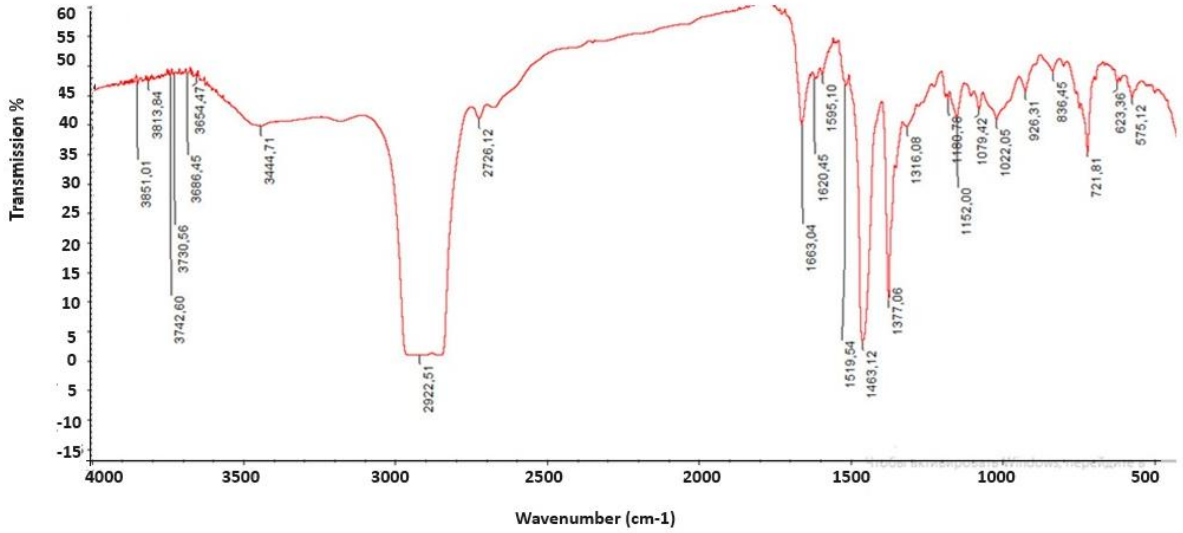

b)

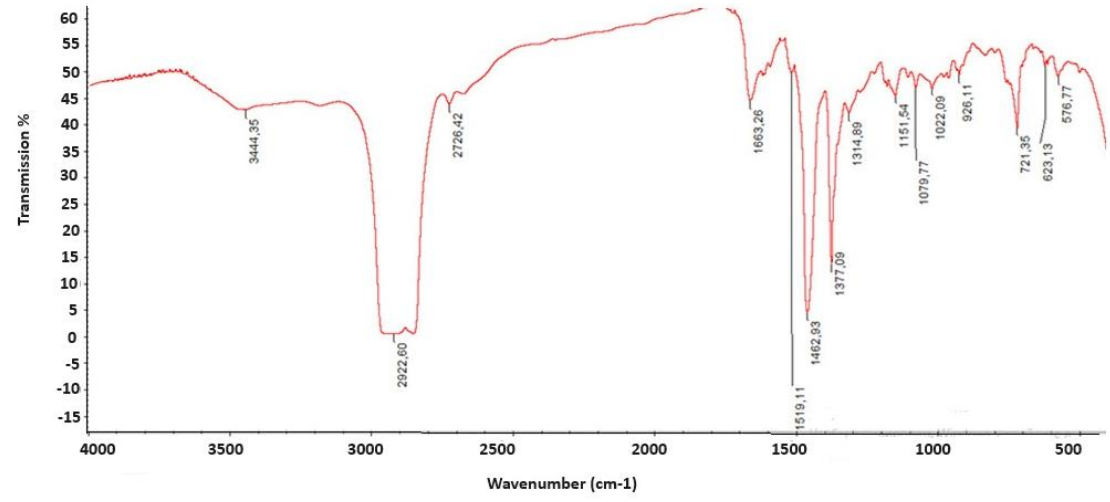

c)

Figure 2. IR spectra of DPC reagent (a), DPC+Ag (b) and DPC+Ag+CTAB (c) complexes.

Figure 3 shows the UV spectra of the DFC reagent (1), DPC+Ag binary complex (2), and DPC+Ag+CTAB ternary complex (3). The UV spectra of silver nanoparticles indicate that the maximum intensity of their absorption bands varies between 400-450 nm, depending on the size of the nanoparticles [22-25]. As can be seen in figure 3 (a), the absorption band of the DFC reagent in the ultraviolet region is located in the range of 205-360 nm, with maximum peaks at 235 nm and 262 nm, corresponding to the π-π* transition of the C-C bond and the n-π* transition between C=N groups. Additional peaks are observed at wavelengths of 308 nm and 345 nm.

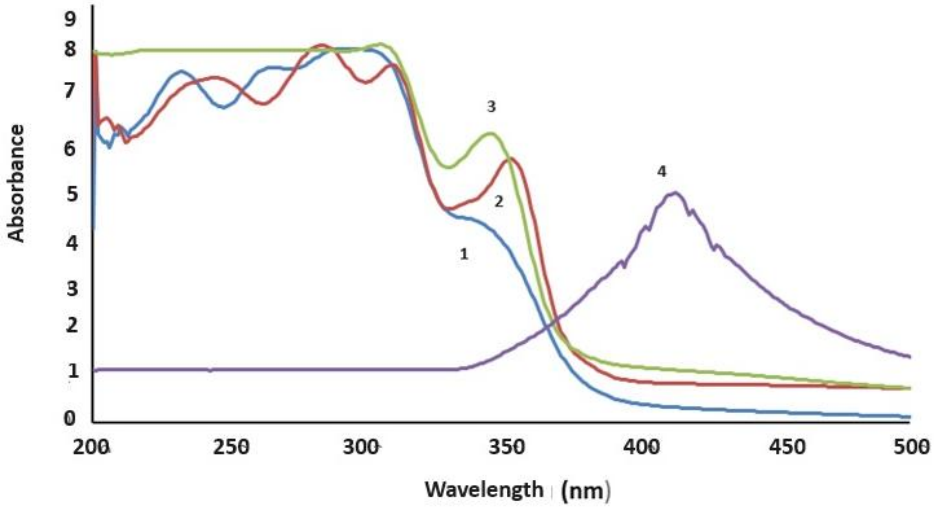

Figure 3. UV spectra of DPC reagent (1), DPC+Ag (2) and DPC+Ag+CTAB (3) complexes, and Ag (4) nanoparticles.

Due to the surface plasmon resonance of the binary complex formed from the addition of 0.01 M silver nanoparticles to the reagent, the absorption curves shift to the right compared to the DPC reagent. This results in the emergence of new maximum peaks at wavelengths of 248 nm, 288 nm, 315 nm, and 355 nm. A bathochromic shift is observed during the formation of the binary complex, indicating a transition to a more acidic environment relative to the DPC reagent. The formation of the Ag+DPC nanocomposite is also accompanied by a noticeable color change from dark red to red. New peaks at longer wavelengths appear due to the aggregation of Ag nanoparticles. The Ag-R-CTAB ternary complex, formed by adding CTAB as a stabilizer to the complex created by the Ag nanoparticles with the DPC reagent, shows changes in the spectrum, with peaks in the absorption band observed at 305 nm and 348 nm. This alteration is attributed to quantum size effects. The formation of a complex with the DPC reagent, involving the coating of Ag nanoparticles with a surfactant, is explained by the generation of new peaks in the absorption band due to surface plasmon resonance and the color change from red to dark brown, which results from the aggregation of Ag nanoparticles. This aggregation also contributes to the bathochromic shift, moving the peak to longer wavelengths.

In figure 3, the displacement of the silver nanoparticles in the UV spectrum relative to the reactants and complexes is associated with the magnitude of the plasmon frequency. Thus, the plasma frequency of silver is greater than that of the binary and ternary complexes.

4. Conclusion

This study explores the synthesis and characterization of new complexes based on silver nanoparticles, diphenylcarbazide (DPC), and cetyltrimethylammonium bromide (CTAB). The novelty of this research lies in the combination of these components to form stable and

spectroscopically distinctive complexes with potential applications in environmental sensing, catalysis, and the determination of metal ions. The observed changes in UV and IR spectra upon complex formation provide insights into the interactions between DPC and AgNPs, making these complexes promising candidates for use in analytical methods, such as photometric detection, and for environmental monitoring systems. The optical and spectral properties of the binary (DPC-AgNP) and ternary (DPC-AgNP-CTAB) complexes, as well as the binding interactions between DFC and AgNPs, were investigated using infrared (IR) and ultraviolet (UV) spectroscopy. The UV spectroscopy results indicate that the DPC reagent exhibits maximum peaks at wavelengths of 235 nm, 262 nm, 308 nm, and 345 nm. In the binary complex, surface plasmon resonance leads to the formation of new maximum peaks at 248 nm, 288 nm, 315 nm, and 355 nm. The ternary complex displays additional peaks at 305 nm and 348 nm, reflecting the structural changes and interactions within the complexes. The infrared spectroscopy results detail the spectral properties of DFC and its complexes, highlighting peaks associated with aromatic C-H and C=C bonds of the phenyl groups, as well as carbonyl (C=O) and C-N bonds of the carbazide group. The shifts in position and intensity of these peaks in the binary and ternary complex spectra indicate the coordination interactions between DFC and AgNPs. In conclusion, these studies underscore the importance of optimizing synthesis methods and exploring new applications to fully harness the potential of AgNPs across various fields of science and industry. By optimizing the synthesis conditions and studying the structural properties, we have created a foundation for the development of AgNP-based complexes that could be applied in various industrial and scientific fields, including sensor technologies, pollution detection, and as catalysts in chemical reactions. The structure and optical properties of the newly synthesized complexes have been determined, and their potential applications have been explored.

Authors' Declaration

The authors declare no conflict of interests regarding the publication of this article.

References

1. W.M. Shume, H.C. Ananda Murthy, E.A. Zereffa, Journal of Chemistry **2020** (2020).
2. M. Gao, L. Sun, Zh. Wang, Y. Zhao, Materials Science and Engineering **33**(1) (2013) 397.
3. K.V. Alex, P.T. Pavai, R. Rugmini, M.S. Prasad, ACS Omega **5**(22) (2020) 13123.
4. S. Shariati, Gh. Khayatian, RSC Advances **11** (2021) 3295.
5. A. Sanchez-Hachair, A. Hofmann, Comptes Rendus Chimie **21**(9) (2018) 890.
6. V. Kumar, D. Singh, S. Mohan, D. Bano, R.K. Gundampati, Journal of Photochemistry and Photobiology B: Biology **168** (2017) 67.
7. M.A. Farooqi, S. Bae, S. Kim, S. Bae, Scientific Reports **14**(1) (2024) 22922.
8. Z.A. Ratan, M.F. Haidere, Md. Nurunnabi, S.Md. Shahriar, Cancers **12**(4) (2020) 855.
9. M.B. Baghirov, M. Muradov, G. Eyvazova, S. Mammadyarova, Y. Azizian-Kalandaragh, N. Musayeva, E.K. Gasimov, F.H. Rzayev, RSC Advances **14** (2024) 16696.
10. K. Kumar, S.R. Anand, M. Kori, N. Mishra, S.P. Shrivastava, Journal of the Indian Chemical Society **100**(4) (2023) 10096.
11. E.G. Karimli, V.N. Khrustalev, M.N. Kurasova, M. Akkurt, A.N. Khalilov, A. Bhattarai, I.G. Mamedov, Acta Crystallographica Section E **79**(5) (2023) 474.
12. F.N. Naghiyev, T.A. Tereshina, V.N. Khrustalev, M. Akkurt, A.N. Khalilov, A.A. Akobirshoeva, I.G. Mamedov, Acta Crystallographica Section E **77**(5) (2021) 512.
13. A.N. Khalilov, J. Cisterna, A. Cárdenas, B. Tuzun, S. Erkan, A.V. Gurbanov, I. Brito. Synthesis, Journal of Molecular Structure **1313** (2024) 138652.
14. M. Akkurt, A.M. Maharramov, N.Q. Shikhaliyev, A. Qajar, G.T. Atakishiyeva, I.M. Shikhaliyeva, A.A. Niyazova, A. Bhattari, UNEC Journal of Engineering and Applied Science **3**(1) (2023) 33.

15. A. Maharramov, N.Q. Shikhaliyev, A. Abdullayeva, G.T. Atakishiyeva, A. Niyazova, V.N. Khrustalev, S.I. Gahramanova, Z. Atioğlu, M. Akkurt, A. Bhattarai, Acta Crystallographica Section E **79**(10) (2023) 905.
16. A. Maharramov, N.Q. Shikhaliyev, A. Qajar, G.T. Atakishiyeva, A. Niyazova, V.N. Khrustalev, M. Akkurt, S.Ö. Yıldırım, A. Bhattarai, Acta Crystallographica Section E **79**(7) (2023) 637.
17. T. Shi, Q. Wei, Zh. Wang, G. Zhang, X. Sun, Q.-Y. He, Molecular Biology and Physiology **4**(3) (2019).
18. N. Aqila, N.H. Aprilita, D. Siswanta, Global NEST Journal **22**(3) (2020) 408.
19. E.A. Badra, S.H. Shafeka, H.H.H. Hefnib, Journal of Molecular Liquids **326** (2021) 115342.
20. H. Wang, G. Zhang, S. Mahmud, R. Mia, H. Liu, Journal of Alloys and Compounds **894** (2022) 162502.
21. E.A. Terenteva, V.V. Apyari, E. Kochuk, S. Dmitrienko, and Yu.A. Zolotov, J Anal Chem **72**(11) (2017) 978.
22. E.A. Terenteva, V.V. Apyari, S.G. Dmitrienko, Yu.A. Zolotov, Spectrochimica Acta Part **151** (2015) 89.
23. M. Pervaiza, S. Sadiqa, A. Sadiq, A. Ashraf, Z. Saeed, Coordination Chemistry Reviews **447** (2021) 214128.
24. J. Swanner, C.D Fahrenholtz, I. Tenvooren, B.W. Bernish , J.J. Sears, A. Hooker, C.M. Furdui, E. Alli, W. Li, G.L. Donati, K.L. Cook, P.-A. Vidi, R. Singh, FASEB Bioadvances **1**(10) (2019) 639.
25. M. Pervaiza, M. Shahina, A. Ejaza, R. Quratulaina, Z. Saeed, A. Ashraf, R.R.M. Khan, S.M. Bukhari, S. Ullah, U. Younas, Inorganic Chemistry Communications **159** (2024) 111851.